Raman spectra of out-of-plane phonons in bilayer graphene

Kentaro Sato,[1] Jin Sung Park,[2] Riichiro Saito,[1] Chunxiao Cong,[3] Ting Yu,[3,4] Chun Hung Lui,[5] Tony F. Heinz,[5] Gene Dresselhaus,[6] and Mildred S. Dresselhaus[7,8]

[1]*Department of Physics, Tohoku University, Sendai 980-8578, Japan*
[2]*Faculty of Engineering, Shinshu University, Nagano 380-8553, Japan*
[3]*Division of Physics and Applied Physics, School of Physical and Mathematical Sciences,*
Nanyang Technological University, 637371, Singapore
[4]*Department of Physics, Faculty of Science, National University of Singapore, 117542, Singapore*
[5]*Department of Physics and Electrical Engineering, Columbia University, 538 West 120th Street, New York, NY 10027, USA*
[6]*Francis Bitter Magnet Laboratory, Massachusetts Institute of Technology, Cambridge, Massachusetts 02139-4307, USA*
[7]*Department of Electrical Engineering and Computer Science, Massachusetts Institute of Technology, Cambridge,*
Massachusetts 02139-4037, USA
[8]*Department of Physics, Massachusetts Institute of Technology, Cambridge, Massachusetts 02139-4307, USA*

The double resonance Raman spectra of the overtone of the out-of-plane tangential optical (oTO) phonon and of combinations of the LO, ZO, and ZA phonons with one another are calculated for bilayer graphene. In the case of the bilayer graphene, these Raman peaks are observed in the energy region between 1600 and 1800 cm^{-1}. We obtain results for both the fixed $q = 0$ and the dispersive $q = 2k$ peaks of the overtones of the oTO phonon of bilayer graphene. We calculate the double resonance Raman spectra of the combination modes coming from the LO, iTO, LA, and iTA phonons in bilayer graphene. The calculated Raman peaks are compared with the experimental results.

I. INTRODUCTION

Resonance Raman spectroscopy has provided unique optical properties for graphitic materials. From an analysis of the Raman spectra, we get rich information on sample characterization and the physical properties of graphene.[1,2] So far, the strong resonance Raman spectra, for example, for the G, D, and G′ (or 2D) bands have been mainly investigated for the purpose of sample characterization of graphene.[3–7] According to double resonance Raman scattering theory,[8] it is expected that many resonance Raman peaks appear in the Raman spectra as overtone or combination modes. Although such Raman peaks have weak intensity compared with that of the G, D, and G′ bands, the information obtained from the Raman spectra is very useful for characterizing the stacking order of multilayer graphene.[9,10]

Graphene is an atomic layer of graphite and a two-dimensional hexagonal lattice of carbon atoms. It is known that the stacking order of multilayer graphene is either ABA (hexagonal) or ABC (rhombohedral).[11] Since some physical properties which are relevant to the interlayer interaction between graphene layers depend on the stacking order, the Raman spectra for the out-of-plane phonon modes are very important for providing information on the difference between single-layer and bilayer graphene and between ABA and ABC stackings. We know that the spectrum of the G′ band become weak and broad with increasing numbers of graphene layers.[5] However, the integrated intensity of the G′ band does not change much with an increase of number of graphene layers. Raman spectra of the out-of-plane modes provide an alternative way for determining the layer numbers.

The out-of-plane tangential optical (oTO) phonon of single-layer graphene at the Γ point in the two-dimensional Brillouin zone is not a Raman active mode due to the odd symmetry

for the mirror operation on a graphene plane. In fact, the Raman peak of the overtone of the oTO phonon of single-layer graphene is not observed. On the other hand, the Raman band of the overtone of the oTO phonon of single wall carbon nanotubes (SWNTs) is observed and is known as the M band,[12,13] since the cylindrical shape of SWNTs makes the M band spectra Raman active. Similarly, the stacking order of multilayer graphene makes the oTO mode Raman active. Recently, some experimental groups observed the Raman spectra in the frequency region between 1600 and 2200 cm^{-1}.[9,10] The Raman frequency depends on the laser excitation energy (E_{laser}) and the number of graphene layers. In the range between 1600 and 2200 cm^{-1}, many weak Raman peaks are observed in the Raman spectra of graphene with different layer thicknesses and the Raman shift depends on E_{laser}.[14] Since the frequencies and intensities of these weak Raman peaks depend on the number of layers of graphene too, it is considered that the out-of-plane phonons around the Γ point are relevant to these weak Raman peaks. Furthermore, the double resonance Raman scattering process occurs within the intravalley scattering process along the phonon energy dispersion in the intermediate frequency region.[12,13]

In this paper, we discuss the calculated Raman shift and intensity of the overtone and combination modes of the out-of-plane phonons around the Γ point in order to evaluate and assign the origin of the weak Raman peaks in the Raman shift range between 1600 and 2200 cm^{-1}. It is known that the interlayer interactions of electrons between the upper and the lower layers of bilayer graphene are weak compared with the intralayer interaction.

In Sec. II, we present the method used for calculating the Raman spectra for bilayer graphene. In Sec. III, we show calculated results for the Raman spectra of the overtone of

TABLE I. The force constants for single-layer graphene in units of 10^4 dyn/cm by Furukawa (Ref. [16]). The subscripts r, ti, and to are radial, transverse in-plane, and transverse out-of-plane, respectively.

Radial	Tangential	
$\phi_r^{(1)} = 39.83$	$\phi_{ti}^{(1)} = 17.13$	$\phi_{to}^{(1)} = 9.39$
$\phi_r^{(2)} = 7.98$	$\phi_{ti}^{(2)} = -4.81$	$\phi_{to}^{(2)} = -0.63$
$\phi_r^{(3)} = -5.53$	$\phi_{ti}^{(3)} = 2.39$	$\phi_{to}^{(3)} = 1.37$
$\phi_r^{(4)} = 1.45$	$\phi_{ti}^{(4)} = 1.85$	$\phi_{to}^{(4)} = -1.28$
$\phi_r^{(5)} = 0.77$	$\phi_{ti}^{(5)} = -0.005$	$\phi_{to}^{(5)} = 0.103$
$\phi_r^{(6)} = -0.519$	$\phi_{ti}^{(6)} = -0.23$	$\phi_{to}^{(6)} = -0.05$
$\phi_r^{(7)} = -1.45$	$\phi_{ti}^{(7)} = -0.50$	$\phi_{to}^{(7)} = 0.70$
$\phi_r^{(8)} = 0.92$	$\phi_{ti}^{(8)} = 3.24$	$\phi_{to}^{(8)} = -0.53$
$\phi_r^{(9)} = -0.20$	$\phi_{ti}^{(9)} = 1.47$	$\phi_{to}^{(9)} = -0.11$
$\phi_r^{(10)} = 0.85$	$\phi_{ti}^{(10)} = -0.43$	$\phi_{to}^{(10)} = 0.00$
$\phi_r^{(11)} = 0.18$	$\phi_{ti}^{(11)} = -2.99$	$\phi_{to}^{(11)} = 0.146$
$\phi_r^{(12)} = -0.56$	$\phi_{ti}^{(12)} = 0.88$	$\phi_{to}^{(12)} = -0.04$
$\phi_r^{(13)} = -0.26$	$\phi_{ti}^{(13)} = -0.81$	$\phi_{to}^{(13)} = -0.05$
$\phi_r^{(14)} = -0.031$	$\phi_{ti}^{(14)} = -0.06$	$\phi_{to}^{(14)} = 0.03$

the oTO phonon and for the combination of the LO, ZA, and ZO phonon modes near the Γ point of bilayer graphene. In addition, we show calculated results for the combination of the LO, iTO, LA, and iTA phonon modes near the Γ point of bilayer graphene. In Sec. IV, a summary is given.

II. CALCULATION METHOD

We use the extended tight binding (ETB) method for calculating the electron energies and the wave function coefficients. The phonon frequency and eigenvectors are calculated by using the force constant models proposed by Furukawa for in-plane modes[16] and by Jishi and Dresselhaus[15] for the out-of-plane modes, which are shown in Tables I and II, respectively.

Here we focus our attention on the optical and acoustic out-of-plane phonons of AB stacked bilayer graphene.[15,17–19] As shown in Fig. 1, there are four out-of-plane phonon modes for bilayer graphene: the out-of-plane acoustic (ZA) and breathing (ZO) modes, and the antisymmetric (oTO⁻) and symmetric (oTO⁺) tangential optic phonon modes. The oTO⁻ phonon is the lower frequency phonon mode at the Γ point around 886.5 cm⁻¹. On the other hand, the oTO⁺ phonon is the higher frequency mode at the Γ point around 887.0 cm⁻¹. The energy difference between the oTO⁻ and oTO⁺ phonons at the Γ point is 0.5 cm⁻¹. The phonon eigenvectors of the lower frequency oTO⁻ phonon are the antisymmetric vibration between the upper and lower layers of bilayer graphene upon

TABLE II. The out-of-plane force constants of graphite by Jishi and Dresselhaus (Ref. [15]). The units are 10^4 dyn/cm.

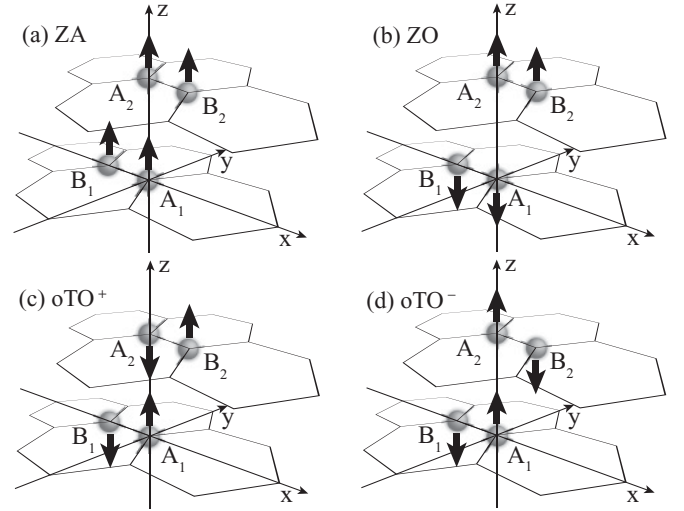| Neighbor	1st	2nd	3rd	4th
Radial	0.27469	0.059552	−0.047388	0.02
Tangential	−0.59341	0.12712	0.04739	−0.09278

FIG. 1. The lattice vibration of the four out-of-plane modes for bilayer graphene. Here the out-of-plane acoustic mode (ZA) (a), the breathing (ZO) mode (b), the symmetric mode (oTO⁺) (c), and the antisymmetric (oTO⁻) (d) tangential optic phonon modes.

the inversion operation at the center point between the A_1 and A_2 atoms. Since the vibration of the oTO⁺ phonon is symmetric, it is expected that the electron-phonon matrix element has a nonzero value in the double resonance Raman scattering process. Since the interlayer interaction is weak, the Raman intensity of the overtone of the oTO phonon is relatively weak compared with the intensities of the G, D, and G′ bands. The other out-of-plane vibrational modes are the ZA and ZO modes. Here the breathing mode (ZO) means that two carbon atoms in the same graphene layer of the unit cell move in phase, while the phase of the vibrations for the two atoms are opposite to each other for the adjacent layers. From the observed Raman shifts between 1600 and 2200 cm⁻¹ and the phonon dispersion relation around the Γ point,[9,14] it is considered that the ZA and ZO phonons can be coupled with the LO and iTO phonons as combination modes. Since the values of the electron-phonon matrix elements of the ZA and ZO phonons are as small as that of the oTO phonon, the Raman intensities of the combinations of the ZA, ZO, LO, and iTO modes are expected to be similarly weak in comparison to the Raman intensity of the overtone of the oTO phonon. Moreover, the Raman peaks of the combination modes of the ZA, ZO, and iTO phonons appear close to the G band frequency and come from the phonon dispersion near the Γ point. We focus our attention on the combination modes of the ZA, ZO, and LO phonons.

The double resonance Raman intensity is calculated by using the following formula:[5,20]

$$I(\omega, E_L)$$
$$= \sum_j \left| \sum_{a,b,\omega_1,\omega_2} \frac{M_{op}(j,c)M_{ph}(c,b)M_{ph}(b,a)M_{op}(a,j)}{\Delta E_{aj}(\Delta E_{aj} - \hbar\omega_1)(\Delta E_{aj} - \hbar\omega_1 - \hbar\omega_2)} \right|^2,$$

(1)

where j, a, b, and c, respectively, denote an initial state in the valence band, an excited state in the conduction band,
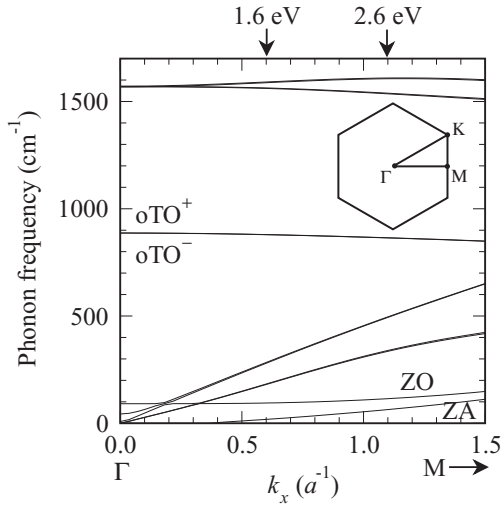
FIG. 2. The phonon dispersion relation of bilayer graphene along the ΓM line. The resonance point arrows for double resonance Raman scattering are also shown, respectively. ΓM $= 2\pi/\sqrt{3}a = 3.63a^{-1}$, where $a = 0.246$ nm is the lattice constant of two-dimensional graphite. The inset is the Brillouin zone of graphene.

a first scattered state, and a second scattered state of an excited electron. Here ΔE_{aj} is the energy separation defined by $\Delta E_{aj} \equiv E_L - (E_a - E_j) - i\gamma$, where γ is a broadening factor and we use a constant $\gamma = 0.01$ eV.[5] Here E_L, E_a, E_j, ω_1, and ω_2 are, respectively, the energies of the excitation laser energy, an initial and excited electron energies, and the two-phonon frequencies. The Raman shift ω is given by $\omega = \omega_1 + \omega_2$. The electron energy and wave function coefficients are calculated based on the ETB method.[21] M_{op} is an electron-photon matrix element between the ground and excited states.[22,23] M_{ph} is an electron-phonon matrix element from an initial state $(a, \boldsymbol{k})$, where $a(\boldsymbol{k})$ is the band index (wave vector), to a final state $(a', \boldsymbol{k}')$ coupled by the νth phonon of the wave vector $\boldsymbol{q}(=\boldsymbol{k} - \boldsymbol{k}')$, the frequency $\omega_\nu(\boldsymbol{q})$, and the phonon eigen vector $\boldsymbol{e}_{\boldsymbol{q}}^\nu$.[24] A force constant model is used for calculating the phonon dispersion.[25] Here we adopt Jishi's force constants for graphite[15] in order to calculate the phonon dispersion of bilayer graphene. Figure 2 shows the resulting calculated phonon dispersion relation along the ΓM line of bilayer graphene, where the M point corresponds to $2\pi/\sqrt{3}a = 3.63a^{-1}$. Here $a = 0.246$ nm is

the lattice constant of two-dimensional graphite. Since we consider only the phonon energy and eigenvector near the Γ point in the Brillouin zone of bilayer graphene, it is assumed that the out-of-plane force constants of bilayer graphene are approximated by those of graphite. We also consider the out-of-plane force constant sets to be multiplied by 1.03 in order to fit the calculated phonon energy to the experimental results. We further assume that the virtual electron state for calculating the electron-photon and electron-phonon matrix elements can be approximated by the initial or final electron states of bilayer graphene.[24] Hereafter, we mainly consider the Raman spectra for AB stacked bilayer graphene.

III. CALCULATED RESULTS AND DISCUSSION

Figure 3(a) shows the calculated results for the double resonance Raman intensity of the overtone of the oTO$^+$ phonon (2oTO$^+$) for the indicated E_{laser} range from 1.6 to 2.6 eV, respectively. It is noted that the calculated Raman intensity for the overtone of the oTO$^-$ phonon (2oTO$^-$) is much smaller [$\sim$0.05 of the tick mark used in Fig. 3(a)] than that for the oTO$^+$ phonon. In the case of the oTO$^-$ phonon, the A$_1$ and A$_2$ (B$_1$ and B$_2$) carbon atoms of the unit cell move in phase, and the phase between the A and B atoms is opposite [see Fig. 1(d)]. Since the out-of-plane vibration of the oTO$^-$ phonon is like the acoustic mode, M_{ph} of the oTO$^-$ phonon is almost zero. On the other hand, in the case of the oTO$^+$ phonon, the A$_1$ and B$_2$ (A$_2$ and B$_1$) carbon atoms of the unit cell move in phase. The out-of-plane vibration of the oTO$^+$ phonon is like the optical mode between the upper and lower graphene layers [see Fig. 1(c)]. This is the reason why M_{ph} for the oTO$^+$ phonon has a nonzero value. Due to the symmetry of the phonon vibration of the oTO phonon, we only find a significant Raman intensity for the 2oTO$^+$ mode in Fig. 3(a).

From the double resonance Raman scattering condition, two Raman peaks, which are called the $q = 0$ and $2k$ peaks, appear through the combination of backward and forward scattering phonons.[8,26] In Fig. 3(a), the left (right) peak corresponds to the $q = 2k$ ($q = 0$) peak for each E_{laser} value. The Raman shift of the $q = 0$ peak does not change by changing the E_{laser},[8] while there is a dispersion observed for the $q = 2k$ peak. Fixed and dispersive peaks of the overtone of the oTO phonon are observed in the Raman shift range between 1730 and 1770 cm^{-1}.
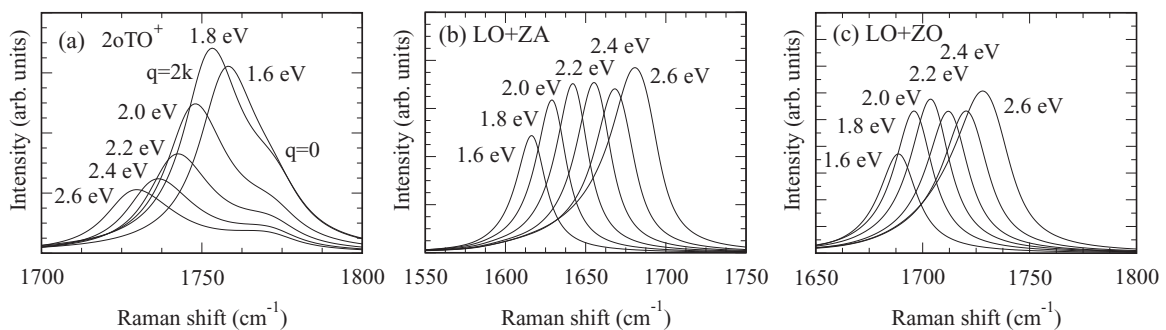

FIG. 3. The Raman spectra of (a) the overtone of the oTO$^+$ phonon (higher energy branch), (b) the combination of the LO and ZA phonons, and (c) the combination of the LO and ZO phonons near the Γ point of bilayer graphene in the laser energy range between 1.6 and 2.6 eV. The Raman intensity for the 2oTO$^+$ combination mode decreases with increasing laser excitation energies above 1.8 eV.
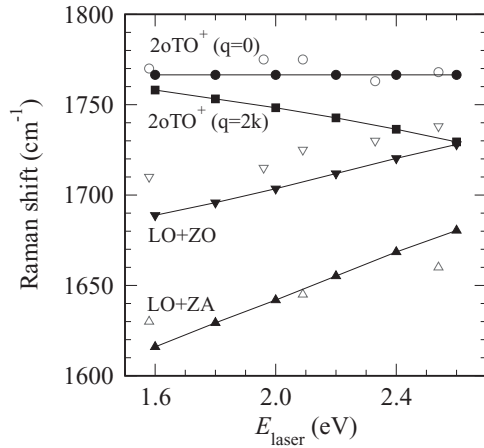
FIG. 4. Raman shifts of combination modes as a function of E_{laser}. Solid (open) symbols are for our calculation [experiment by Lui *et al.* (Ref. 14)]. The symbols denote $2oTO^+$ ($q = 0$) (circles), $2oTO^+$ ($q = 2k$) (squares), LO + ZA (up triangles), and LO + ZO (down triangles), respectively.
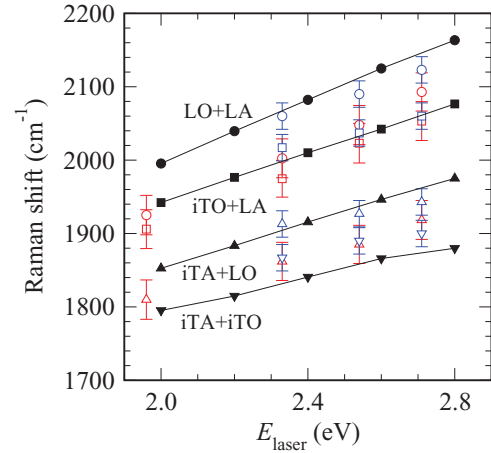

FIG. 5. (Color online) The relation between E_{laser} and the Raman shifts. Black solid (blue open) symbols are for the calculation (experiment) for bilayer graphene. Red open symbols are for the experiment by Cong *et al.* for single-layer graphene.[9] The symbols denote LO + LA (circles), iTO + LA (squares), iTA + LO (up triangles), and iTA + iTO (down triangles), respectively.

In Fig. 3(a), we can see that the Raman intensity of the $2oTO^+$ decreases with increasing E_{laser} because M_{el-ph} depends on the reciprocal lattice vector and M_{el-ph} decreases with increasing distance from the K point.[22,23] Furthermore, the difference in the Raman shift between the $q = 0$ and $2k$ peaks increases with increasing E_{laser}. Figures 3(b) and 3(c) show the corresponding calculated results for the double resonance Raman intensity of the combination of the LO and ZA phonons (LO + ZA) and the LO and ZO phonons (LO + ZO) as a function of E_{laser} from 1.6 to 2.6 eV, respectively. There is a dispersive peak for each Raman shift in the range between 1610 and 1730 cm^{-1}. Both the Raman intensity and the frequency shift for LO + ZO and LO + ZA increase with increasing E_{laser}, because the LO intensity increases with increasing E_{laser}.

Figure 4 shows the Raman shifts of Fig. 3 as a function of E_{laser}. Solid (open) symbols are for the calculation (experiment by Lui *et al.*[14]). Here we show the results for $2oTO^+$ ($q = 0$) (circles), $2oTO^+$ ($q = 2k$) (squares), LO + ZA (up triangles), and LO + ZO (down triangles) modes, respectively. The dispersion of the calculated Raman spectra for the $2oTO^+$ ($q = 0$), LO + ZO, and LO + ZA combination modes reproduces the experimental result well. However, there is no correspondence between the calculation and the experiment for the negative dispersive ($q = 2k$) peaks of $2oTO^+$ which appear in the Raman shift range from 1730 to 1760 cm^{-1}. This dispersive peak intersects LO + ZO at $E_{laser} = 2.6$ eV in Fig. 4. Thus, it is considered that this intersection of $2oTO^+$ ($q = 2k$) with the LO + ZO combination mode affects both the peak intensities and the widths of the LO + ZO mode at the crossing points. The experimental Raman intensities are not strong in this spectral range. The assignment of the $2oTO$ ($q = 2k$) mode remains to be confirmed by future experiments.

Next we show in Fig. 5 the Raman shifts for four possible combinations of the LO, iTO, LA, and iTA phonons as a function of E_{laser} using the same strategy as in Fig. 4. From the experimental Raman spectra and phonon dispersion results of

single- and bilayer graphene, it is considered that the origin of the Raman peaks in Fig. 5 is the combination of the LO and LA phonons (LO + LA) (circles), the combination of the iTO and LA phonons (iTO + LA) (squares), the combination of the iTA and LO phonons (iTA + LO) (up triangles), and the combination of the iTA and iTO phonons (iTA + iTO) (down triangles) within the intravalley scattering process, respectively. Here we consider and calculate the Raman spectra of the above combination modes of bilayer graphene in order to demonstrate the origin of these peaks. Black solid (blue open) symbols are for calculated values (experiments by Cong *et al.*[9]) for the bilayer graphene in Fig. 5. Red open symbols are for the experiment of single-layer graphene by Cong *et al.*[9] The results for the energy dependence of the calculated dispersion curve are $\omega_{LO+LA} = 211$, $\omega_{iTO+LA} = 167$, $\omega_{iTA+LO} = 154$, and $\omega_{iTA+iTO} = 110$ cm^{-1}/eV, respectively. The values for the dispersion in these peaks tend to agree with the experiment. The Raman shift increases with increasing E_{laser} due to the phonon dispersion around the Γ point. Moreover, a phonon energy difference between the LA and iTA (LO and iTO) modes can be determined from Fig. 5. In the experimental Raman spectra, there is another Raman peak in the range from 1800 to 2200 cm^{-1}. We expect that the weak Raman peak LA + iTA corresponds to the intervalley scattering process appearing in the range from 1800 to 2200 cm^{-1}. The Raman intensity calculation for the intervalley scattering process is beyond the scope of this paper.

IV. SUMMARY

In summary, we show calculations for the double resonance Raman spectra for the overtones of the oTO phonons and for the combinations of the ZA, ZO, and LO phonons for bilayer graphene. These double resonance peaks are not observed in the Raman spectra from single-layer graphene. However, due to the lattice vibration symmetry of bilayer graphene, weak Raman peaks appear in the Raman spectra

between 1600 and 1800 cm^{-1}. Fixed $q = 0$ and dispersive $q = 2k$ Raman peaks appear in the Raman spectra of the overtones of the oTO phonon. Moreover, we show calculated results for the Raman spectra of the combination modes coming from the LO, iTO, LA, and iTA phonons in bilayer graphene.

[1] L. M. Malard, M. A. Pimenta, G. Dresselhaus, and M. S. Dresselhaus, Phys. Rep. **473**, 51 (2009).

[2] A. H. Castro Neto, F. Guinea, N. M. R. Peres, K. S. Novoselov, and A. K. Geim, Rev. Mod. Phys. **81**, 109 (2009).

[3] F. Tuinstra and J. L. Koenig, J. Chem. Phys. **53**, 1126 (1970).

[4] C. Casiraghi, S. Pisana, K. S. Novoselov, A. K. Geim, and A. C. Ferrari, Appl. Phys. Lett. **91**, 233108 (2007).

[5] J. S. Park, A. Reina Cecco, R. Saito, J. Jiang, G. Dresselhaus, and M. S. Dresselhaus, Carbon **47**, 1303 (2009).

[6] E. H. Martins Ferreira, M. V. O. Moutinho, F. Stavale, M. M. Lucchese, R. B. Capaz, C. A. Achete, and A. Jorio, Phys. Rev. B **82**, 125429 (2010).

[7] K. Sato, R. Saito, Y. Oyama, J. Jiang, L. G. Cançado, M. A. Pimenta, A. Jorio, G. G. Samsonidze, G. Dresselhaus, and M. S. Dresselhaus, Chem. Phys. Lett. **427**, 117 (2006).

[8] R. Saito, A. Jorio, A. G. Souza Filho, G. Dresselhaus, M. S. Dresselhaus, and M. A. Pimenta, Phys. Rev. Lett. **88**, 027401 (2001).

[9] C. Cong, T. Yu, R. Saito, G. F. Dresselhaus, and M. S. Dresselhaus, ACS Nano **5**, 1600 (2011).

[10] R. Rao, R. Podila, R. Tsuchikawa, J. Katoch, D. Tishler, A. M. Rao, and M. Ishigami, ACS Nano **5**, 1594 (2011).

[11] N. B. Brandt, S. M. Chudinov, and Y. G. Ponomarev, *Graphite and its Compounds*, Modern Problems in Condensed Matter Physics Vol. 20.1 (Elsevier Science Ltd., Amsterdam, 1988).

[12] V. W. Brar, G. G. Samsonidze, M. S. Dresselhaus, G. Dresselhaus, R. Saito, A. K. Swan, M. S. Ünlü, B. B. Goldberg, A. G. Souza Filho, and A. Jorio, Phys. Rev. B **66**, 155418 (2002).

[13] S. D. M. Brown, P. Corio, A. Marucci, M. A. Pimenta, M. S. Dresselhaus, and G. Dresselhaus, Phys. Rev. B **61**, 7734 (2000).

[14] C. H. Lui, L. M. Malard, S. Kim, G. Lantz, F. E. Laverge, R. Saito, and T. F. Heinz (unpublished).

[15] R. Al Jishi and G. Dresselhaus, Phys. Rev. B **26**, 4514 (1982).

[16] M. Furukawa, Master's thesis, Tohoku University, 2010.

[17] K. H. Michel and B. Verberck, Phys. Rev. B **78**, 085424 (2008).

[18] N. Mounet and N. Marzari, Phys. Rev. B **71**, 205214 (2005).

[19] L. Karssemeijer and A. Fasolino, Surf. Sci., 10.1016/j.susc.2010.10.036 (to be published 2010) (Corrected Proof).

[20] M. S. Dresselhaus, G. Dresselhaus, R. Saito, and A. Jorio, Phys. Rep. **409**, 47 (2005).

[21] G. G. Samsonidze, R. Saito, N. Kobayashi, A. Grüneis, J. Jiang, A. Jorio, S. G. Chou, G. Dresselhaus, and M. S. Dresselhaus, Appl. Phys. Lett. **85**, 5703 (2004).

[22] A. Grüneis, R. Saito, G. G. Samsonidze, T. Kimura, M. A. Pimenta, A. Jorio, A. G. SouzaFilho, G. Dresselhaus, and M. S. Dresselhaus, Phys. Rev. B **67**, 165402 (2003).

[23] J. Jiang, R. Saito, A. Grüneis, G. Dresselhaus, and M. S. Dresselhaus, Carbon **42**, 3169 (2004).

[24] J. Jiang, R. Saito, G. G. Samsonidze, S. G. Chou, A. Jorio, G. Dresselhaus, and M. S. Dresselhaus, Phys. Rev. B **72**, 235408 (2005).

[25] R. Saito, G. Dresselhaus, and M. S. Dresselhaus, *Physical Properties of Carbon Nanotubes* (Imperial College Press, London, 1998).

[26] L. G. Cançado, M. A. Pimenta, R. Saito, A. Jorio, L. O. Ladeira, A. Grüeneis, A. G. Souza-Filho, G. Dresselhaus, and M. S. Dresselhaus, Phys. Rev. B **66**, 035415 (2002).